Design rules for adaptive turbo equalization in fast-fading channels

Land, Ingmar Rüdiger; Collings, I. B.; Peacock, M. J.

Published in:
IASTED Int. Conf. Commun. Systems and Networks, September 2002

Publication date:
2002

Document Version
Publisher's PDF, also known as Version of record

Design Rules for Adaptive Turbo Equalization in Fast-Fading Channels

Matthew J. M. Peacock* and **Iain B. Collings**
School of Electrical & Information Engineering
The University of Sydney
Sydney, NSW, 2006, AUSTRALIA.
email: {mpeac,iain}@ee.usyd.edu.au

Ingmar Land
Information & Coding Theory Lab
Faculty of Engineering, University of Kiel
Kaiserstr. 2, D-24143, Kiel, GERMANY
email: il@tf.uni-kiel.de

Abstract

This paper uses the mutual information (MI) transfer metric to characterize the behavior of an adaptive turbo equalization scheme. We consider recursive systematic convolutional coding at the input to a multipath fast-fading channel. The equalizer is a recent adaptive, near-optimal APP algorithm that incorporates MMSE channel estimation. We develop design rules for this turbo equalizer using EXIT charts. We optimize the use of pilot bits and determine the best ratio of code bits to pilot bits, for fixed data and symbol rates.

Keywords: Turbo Equalization, EXIT charts, Fading Channels

1 Introduction

Recent interest in near-optimal adaptive equalizers has been fuelled by the continual exponential growth of emerging DSP technologies. Advanced equalizers include per-survivor processing (PSP) [1], pilot-symbol aided modulation (PSAM) with soft-output Viterbi equalization [2], expectation-maximization techniques [3], trellis-expanded APP [4], and a variety of iterative techniques often called turbo-equalization, which iterate between equalization and decoding stages using soft inputs and outputs eg. [5].

Most current turbo equalization schemes assume the channel is known at the receiver. However, a recent modification [4] of the A-Posteriori Probability (APP) algorithm [6] is a near-optimal fractionally-spaced equalizer for fast-fading channels which expands the equalizer trellis to include MMSE channel estimation. The equalizer accepts *a priori* (soft) inputs and gives *a posteriori* (soft) outputs, and hence can be incorporated into a turbo processing loop. For clarity, we will refer to this equalizer as the Trellis-Expanded A-Posteriori Probability (TE-APP) equalizer. In a turbo structure, so-called extrinsic information is passed between stages. In essence this is the extra (soft) information the equalizer/decoder generates about a data bit which was not present prior to that stage.

Unfortunately, iterative equalization schemes are notoriously complex, and difficult to analyze mathematically. Recently in the field of turbo coding **EX**trinsic **I**nformation **T**ransfer (or EXIT) charts have been proposed [7] as a new analysis tool. EXIT charts have recently been used to determine a stopping criterion for iterative decoding [8], and have also been applied to turbo equalization schemes over fixed multipath channels [9]. The main idea of EXIT chart characterization is to consider the constituent decoders/equalizers individually in a 'black box' fashion, and then consider the interplay between the two.

This paper applies the EXIT chart approach to characterize the TE-APP equalizer and determines a number of key design factors for turbo equalization with unknown channel state information (CSI). We analyze performance as a function of fading rate, SNR, pilot rate, and code rate. We develop design rules for optimizing the choice of pilot and code puncturing rates, in order to ensure convergence while minimizing the number of turbo iterations. We do this under conditions of constant data rates, and without changing the modulation format or symbol rates. We also provide simulated BER curves to verify the conclusions we draw from the EXIT charts. Of course EXIT charts require significantly less computations than BER curves.

2 Transmission and Channel Model

Consider the communication system depicted in Fig. 1 where a data block of N_b bits $\{b_i\}$ is encoded using a outer recursive systematic convolutional code (RSCC) of rate R_c to obtain the sequence $\{v_j\}$ of $N_c = N_b/R_c$ coded bits. The parity bits from the coded sequence are punctured at a rate $1{:}K$, i.e. every $(K+1)^{\text{th}}$ parity bit is removed to obtain N_p punctured coded bits. This sequence is then interleaved using an S-rand interleaver [10] and interspersed with pilot bits with frequency $1{:}P$ to give $N_p\frac{P+1}{P}$ total bits. Using pilot bits rather than whole symbols is a slightly more flexible approach than direct PSAM, as for turbo equalization we do not need entire pilot symbols, which will be discussed in section 4. Finally, this sequence is modulated into a sequence of 2^q-ary symbols of length N, where

$$N \simeq \frac{N_b}{q}\left(\frac{P+1}{P}\right)\left(1+\left(\frac{K}{K+1}\right)\left(\frac{1}{R_c}-1\right)\right) \quad (1)$$

where the approximation comes about because in practice each fraction must be converted to the appropriate

*Matthew Peacock is supported in part by the Australian CSIRO

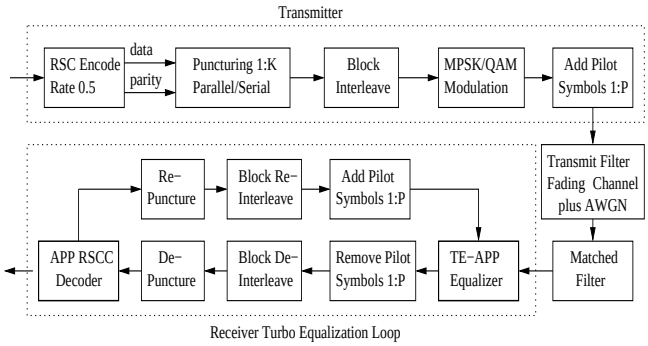

Figure 1. Block diagram of Transmitter, Channel and Iterative Receiver

integer.

Assume the N channel symbols are transmitted with symbol period T. The input to the transmit pulse shaping filter will be denoted

$$x(t) = \sum_{n=0}^{N-1} u_n \delta(t - nT) \tag{2}$$

where u_n is the n^{th} 2^q-ary channel symbol and $\delta(\tau)$ is the continuous time Dirac delta function. Assume that the channel has a fixed number M of WSSUS Rayleigh-fading echoes with time-varying random unknown amplitude but with known average power, eg. as given in [11]. Normalized coherence time is defined as $T_c = f_{D_{\max}} T$, where $f_{D_{\max}}$ is the maximum doppler spread of the channel. The time-varying impulse response of the channel is therefore

$$h(t;\tau) \quad = \quad \sum_{m=0}^{M-1} c_m(t)\delta(\tau - \tau_m(t)) \tag{3}$$

where $c_m(t)$ and $\tau_m(t)$ are the complex gain and delay of the m^{th} path at time t respectively. Also let $E[c_m(t)c_m^*(t)] = \rho_m$. Incorporating the transmit pulse shaping filter and a fixed matched filter receiver (eg. root-raised cosine filters) gives

$$\begin{aligned} f(t;\tau) &= g(\tau) * h(t;\tau) * g^*(-t) \\ &= \sum_{m=0}^{M-1} c_m(t) g_{\text{tot}}(\tau - \tau_m) \end{aligned} \tag{4}$$

where $g(\tau)$ is the pulse shaping filter impulse response and $g_{\text{tot}}(\tau)$ denotes the combined transmit/receive filter response $g(\tau) * g^*(-\tau)$. The received signal will be denoted

$$z(t) \quad = \quad f(t;\tau) * x(t) + n(t) \tag{5}$$

where $n(t)$ is an additive white Gaussian noise process with 2-sided spectral noise density $N_0/2$.

Since the pulse-shaping filter introduces bandwidth expansion, we must oversample the received signal with period $T_s = TR$, $R \leq 1$ to obtain $\{z_k\}$, $z_k \triangleq z(t = kT_s)$. As is common, also assume that the pulse shape is shifted and truncated to become finite and causal, such that the resulting effective impulse response of the combined channel and filters has duration $\leq \ell T_s$.

3 Adaptive Turbo Equalizer Structure

We consider the turbo equalization loop shown in Fig. 1 which is in the style of [5, 12, 13].

First consider the TE-APP equalizer [4], which jointly estimates the channel response and the data sequence, creating a different channel estimate for each transition in the equalizer trellis (similar to PSP, but in the case of soft APP outputs). The state-space of the trellis is expanded to include an additional G symbols and g additional samples for the purpose of channel estimation. This is achieved with a MMSE linear predictor. For details, see [4].

It is possible to generalize the scheme to M-ary signal constellations by converting the symbol APP outputs of the TE-APP equalizer into a string of bit LLRs

$$\begin{aligned} L_e^{\text{equ}}(v'_{qn+\nu}) \quad &= \quad \ln\left(\frac{\sum_{s=0}^{2^q-1} \text{APP}_s(u_n)\,\kappa_1^\nu(s)}{\sum_{s=0}^{2^q-1} \text{APP}_s(u_n)\,\kappa_0^\nu(s)}\right) \\ &\text{for } \nu \in \{0,\ldots,q-1\},\ \ n \in \{0,\ldots,N-1\} \end{aligned} \tag{6}$$

where $L_e^{\text{equ}}(v'_j)$ is the extrinsic information yielded from the equalizer about the $(v'_j)^{\text{th}}$ channel bit. The sequence $\{v'_j\}$ contains pilot bits, and otherwise is the punctured, interleaved coded bit sequence. The term $\text{APP}_s(u_n)$ is the *a posteriori* probability of the n^{th} channel symbol is the constellation point s. Also $\kappa_1^\nu(s)$ is 1 when the ν^{th} bit of constellation point s is '1' and 0 otherwise, and $\kappa_0^\nu(s)$ is the logical inverse of $\kappa_1^\nu(s)$.

Similarly in the feedback path, the bit LLRs must be converted into symbol APPs. It can easily be shown this amounts to computing

$$\text{APP}_s(u_n) = \prod_{\nu=0}^{q-1} \frac{\kappa_0^\nu(s) + e^{L_e^{\text{dec}}(v_{qn+\nu})}\kappa_1^\nu(s)}{1 + e^{L_e^{\text{dec}}(v_{qn+\nu})}} \tag{7}$$

where $L_e^{\text{dec}}(v_j)$ is the extrinsic information yielded from the decoder about the v_j^{th} coded bit.

For the decoder, we use the standard APP algorithm to decode the convolutional code with soft inputs and outputs [6]. The overall decoder LLR of each coded bit v_j given the sequence of pilot-free, de-interleaved, and depunctured extrinsic LLRs from the output of the equalizer ($\mathbf{L}_0^{N_c-1}$) is

$$L^{\text{dec}}(v_j) = \ln \frac{P(v_j = 1|\mathbf{L}_0^{N_c-1})}{P(v_j = 0|\mathbf{L}_0^{N_c-1})} \tag{8}$$

for $j \in \{0,\ldots,N_c-1\}$.

In the turbo equalizer, the extrinsic decoder LLRs are extracted from (8) and passed back to the TE-APP equalizer as *a priori* inputs. This iteration continues until convergence. If the turbo equalizer is designed properly, this convergence will be at a point of zero errors. Such a design is the topic of this paper.

4 Design Tradeoff Issues

One of the main tradeoffs when designing adaptive turbo equalizers for fast fading channels is how much redundancy to introduce into the data stream. Of course redundancy is needed to correct errors as well as to assist with

channel estimation. It can be added in either the coder by reducing the code rate, or after the interleaving by adding pilot bits.

First consider the pilot rate in relation to the channel fading rate. The PSAM technique demonstrated that by adding pilot symbols at at least twice the rate of fading, accurate channel estimates can be generated by interpolation, although it is limited to the case of flat fading. With APP-based turbo equalization, pilots can be added into the data stream rather than the modulated symbol stream, allowing the equalization trellis to be collapsed, which in turn assists with channel estimation. Clearly this is a different technique to PSAM, and as such there is no obvious way to determine the optimal pilot rate. In fact, we will show that a significantly reduced pilot rate compared to PSAM can be used, including for ISI channels, thus resulting in higher transmission efficiency. We use EXIT charts for this optimization.

In addition there is a design tradeoff between pilot rate and code rate. Of course if we add more pilot symbols to aid channel estimation then we will need to use a higher rate code in order to maintain a constant overall data rate. This will hence make the decoding less powerful. So accuracy in the equalizer is traded off against correction capability in the decoder. The table below shows an example where we increase the code rate by puncturing the code at rate K, and introduce pilot bits at rate P. The table shows a selection of P,K combinations that give a fixed redundancy of 1/2 when puncturing a code of rate $R_c = 1/2$.

P	3	7	11	15	19	23	31	55	100
K	1	3	5	7	9	11	15	27	50

At one extreme, almost all redundancy is put into the code with very infrequent pilot bits (K,P large). In this case the turbo equalizer relies heavily on the code to feedback significantly improved *a priori* information to the TE-APP equalizer. At the other extreme, the turbo equalizer is expected to obtain excellent symbol estimates due to the frequent pilot bits and then uses a heavily punctured code to fix a small number of remaining errors (K,P small). To date, there is no analysis which can tell us which of these combinations performs the best. In this paper, we use EXIT charts to derive MI based performance measures to examine this tradeoff.

5 EXIT Charts

To create an EXIT chart, we need to consider mutual information transfer (MIT) curves. The mutual information is measured between the extrinsic probabilities and the true data sequence. An MIT curve for an equalizer or decoder is obtained by applying several *a priori* inputs with known MI and determining the MI at the *a posteriori* output. An EXIT chart is generated by plotting the decoder MIT curve over the top of the equalizer MIT curve, but with the axes swapped. This is done since the *a posteriori* output of the decoder becomes the *a priori* input to equalizer and vice versa. Hence, the iterative scheme can be visualized to be a staircase working its way between the two curves. When the curves intersect, on average this will be the point where the iterative decoding/equalization will cease to enhance the MI between the extrinsics and the data sequence.

In [7] it was shown for AWGN channels that the *a priori* input to the decoder/equalizer can be modelled by applying an independent Gaussian random variable n_A with variance σ_A^2 and mean zero in conjunction with the known transmitted systematic bits x. To obtain a MIT characteristic of the decoder, the *a priori* input for coded bit $v_j \in \{0, 1\}$ is modelled as

$$L_{ap}(v_j) = \mu_A(2v_j - 1) + n_A(j) \tag{9}$$

where the $n_A(j) \sim N(0, \sigma_A^2)$ are mutually independent. It has been shown [7] that μ_A must fulfil $\mu_A = \frac{\sigma_A^2}{2}$. In this paper where we consider fast-fading ISI channels, we have found that this is also a valid model for the *a priori* inputs.

Hence we can analytically determine the MI $I_A = I(X; A)$ between the transmitted systematic bits X and the *a priori* inputs [7]

$$I_A(\sigma_A^2) = 1 - \int_{-\infty}^{\infty} \frac{\exp\left(-\frac{(\xi-\mu_A)^2}{2\sigma_A^2}\right)}{\sqrt{2\pi\sigma_A^2}} \cdot \log_2(1 + e^{-\xi}) d\xi \tag{10}$$

Note that since I_A is a monotonically increasing function of σ_A^2, it is reversible. This must be used during simulation when stepping through the input MI from zero to one. For each value of input MI, $I_A(\sigma_A^2)$ must be reversed to find the appropriate value of σ_A^2.

To determine the MI between the data sequence and the extrinsic information at the output of decoder/equalizer, we require the conditional p.d.f. $p_E(\xi|B_i = b_i)$. In this paper we determine this p.d.f. by Monte Carlo simulation (histogram measurements) of the TE-APP equalizer and the APP decoder.

6 Simulation Results

Unless stated otherwise, for all simulations we have considered a turbo equalization scenario with the following parameters.

- Recursive convolutional code of rate 0.5, memory 4 given by $(G_r, G) = (023, 037)_8$ where G_r is the feedback polynomial with most significant bit corresponding to the leftmost (input) connection.
- Minimal separation parameter $S = \frac{1}{3}\sqrt{\frac{N}{2}}$ in the S-random interleaver.
- BPSK modulation
- $N = 10^4$ channel symbols per block
- Oversampling rate $R = 0.5$
- Root-raised cosine pulse shaping filter with rolloff factor $\beta = 0.5$
- Two path fading model with equal average power and relative delay one symbol period.
- Truncation of pulse shaping filter to extend for a total of 5 symbol intervals. Effective number of total channel taps after considering multipath $\ell = 12$

- Normalized channel coherence time $T_c' = \frac{T_c}{T} = 20$ symbols (i.e. fast fading).

6.1 Mutual Information Transfer (MIT) Characteristics and EXIT Charts

We start by examining the decoder performance within the turbo equalizer structure. Fig. 2 shows the extrinsic MI transfer characteristics of the memory 4 code with various puncturing rates. Recall that the output extrinsics are fed back to the TE-APP equalizer as *a priori* inputs for the next turbo iteration. As can be seen, these feedback extrinsics will not be significant unless the decoder receives extrinsic inputs which have an MI of at least 0.3. If the feedback extrinsics are not significantly better than the original *a priori* inputs, then the turbo equalizer may not enhance the original data estimate.

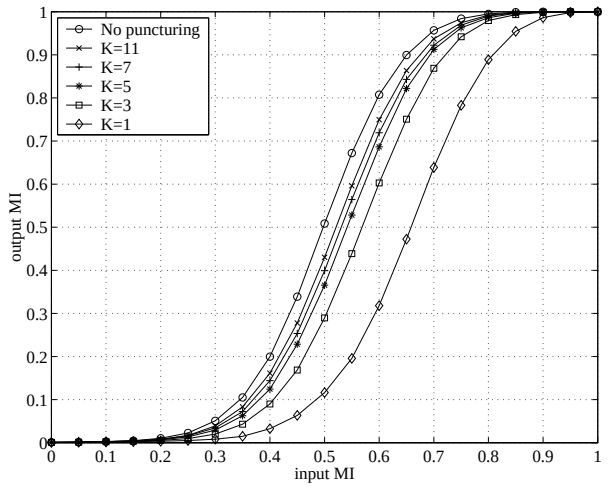

Figure 2. Mutual Information Transfer Characteristics of a punctured RSCC of memory 4

Fig. 3 shows the MI transfer characteristics of the TE-APP equalizer for different values of SNR and pilot bit rates. It also shows the curves for APP equalization with full CSI. Note that even for high input MI, the maximum output MI value obtained is not equal to 1, as was observed in [9] where they considered known, fixed ISI channels. It is interesting to note that in our pilot-aided case of fast fading channels with unknown CSI, the pilot bit rate only affects the MIT curve for low input MI. In addition, the maximum output MI value is independent of the pilot rate and depends only on the received SNR (and the fading rate, as seen in Fig. 4). Of course as expected, with increased SNR the output MI curves are raised, indicating improved performance of the TE-APP equalizer.

Fig. 4 shows the MI transfer characteristics of the TE-APP equalizer for two different fading rates and 3 different pilot rates. As expected, the TE-APP equalizer performs better at the slower fading rate, achieving a higher maximum output MI. Faster fading rates lead to lower maximum output MI. Although it is not the same, in terms of these MIT curves it is somewhat equivalent to an SNR penalty. This is seen by observing that the curves in Fig. 3 and Fig. 4 have similar properties, even though one is generated from variations in SNR and the other from variations in fading rate.

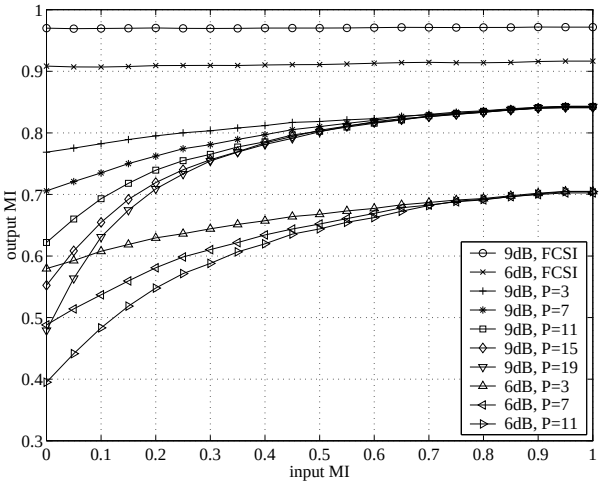

Figure 3. Mutual Information Transfer Characteristics of Full-CSI and TE-APP equalizers at different SNRs

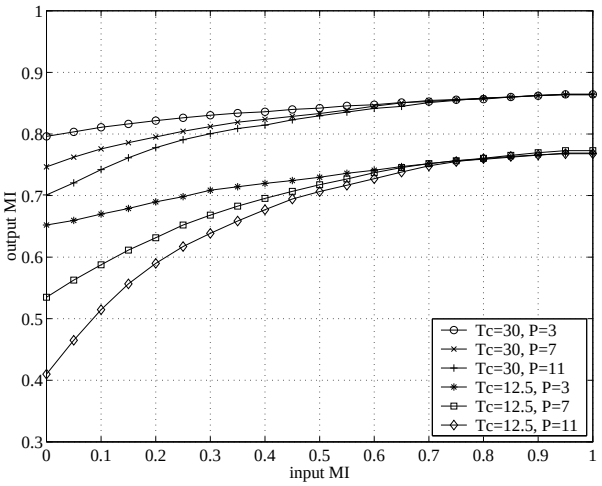

Figure 4. Mutual Information Transfer Characteristics of the TE-APP equalizer under different fading rates at 9dB SNR

Fig. 5 shows an EXIT chart for the full turbo equalizer, (i.e. the axes of the code MIT curve are flipped and overlaid on the TE-APP equalizer MIT curve). The figure also shows a simulated MI trajectory for a realization of the turbo equalizer. Note that the MI transfer curves accurately predict the decoding behavior for a fading channel, in this case of unknown CSI. Clearly the wider the gap between the two curves, the less iterations will be required.

6.2 Redundancy Allocation

Fig. 6 shows EXIT charts for the full turbo equalizer, (i.e. the axes of the code MIT curve are flipped and overlaid on the TE-APP equalizer MIT curve). The figure shows pairs of equalizer/decoder curves which have the appropriate combinations of pilot bits and puncturing so that

in each case the overall data rate is the same (as shown in the table in section 4).

Note that there are two crucial regions where the turbo equalizer can fail to converge. The first crucial region is early in the iterations (i.e. low MI region). The figure shows that the $P = 100$, $K = 50$ pair of curves cross at an equalizer output MI value of 0.16. In this case, we see that the pilot bits are clearly too infrequent, relative to fading rate and SNR. Hence there are too many errors remaining at the TE-APP equalizer output for the decoder to correct, even though it has a relatively large puncturing value K.

Another interesting point is that for the fading rate in Fig. 6, standard PSAM would require pilots at a rate of $P = 10$ to accurately interpolate the channel estimates (due to Nyquist), whereas it is clear from our EXIT chart that the TE-APP equalizer will work even at the highly infrequent rate of $P = 55$. Therefore it is more efficient.

The second crucial region on the EXIT chart is in the high MI range. Clearly, because the equalizer curves do not approach 1, as discussed earlier, it is important that the equalizer MIT curve does not intersect the decoder MIT curve until it reaches the extreme right-hand axis. Once it has reached the extreme right-hand axis, the decoder curve will take the MI to 1, at the next iteration. As discussed in relation to Fig. 3, this crossing point is independent of the pilot bit rate, and depends only on the received SNR and the code and puncturing properties.

In summary, Fig. 6 demonstrates that for this channel, convergence will be achieved for all pilot/puncturing scenarios shown except for the two extreme cases. The final design choice is to ensure minimum number of iterations, which is typically found by selecting the pair with the largest gap between the curves, as discussed in relation to Fig. 5. In this case of Fig. 6, we choose the combination $P = 7$, $K = 3$.

6.3 BER Verification

In this section we provide BER plots which verify the validity of EXIT chart analysis for this time varying, unknown CSI, turbo equalizer. Fig. 7 shows the simulated BER curves for two sets of pilot/puncturing combinations. First, from the EXIT chart of Fig. 6, we conclude that on average the $P = 7$, $K = 3$ combination will converge to zero errors at SNR=10.5dB since the TE-APP equalizer curve reaches the right-hand axis before it crosses the decoder curve. Clearly this is not the case for the $P = 3$, $K = 1$ combination. We also note from the trajectory in Fig. 5 that on average we would expect that 2 iterations will be enough to converge. Each of these predictions is confirmed in the BER plot of Fig. 7 by looking at the values at 10.5dB SNR.

In fact the knee in the BER curve can be predicted from our EXIT charts. By overlaying the 6dB SNR TE-APP equalizer MIT curve from Fig. 3 over the decoder MIT curve in an EXIT chart we see that the crossing point is at a high MI value. Due to the steep slope of the decoder MIT curve, it only requires a reduction in SNR to 4dB for the crossing point to move to a significantly lower MI, although we do not have room to show this. Therefore we would expect the BER knee to be at 4dB as confirmed by Fig. 7.

6.4 Design Rules

In light of our above observations, we now provide a set of design rules for turbo equalization with unknown CSI, which will result in the minimum number of iterations on average for a fixed overall data rate and symbol rate.

- First determine the worst-case received SNR-fading rate scenario under which the system is expected to operate.
- For this noise-fading scenario, evaluate the equalizer's output MI for an input MI of 1, and call this $\mathrm{MI}_{\mathrm{equ}}^{\max}$. We start the design here since we have found this value to be independent of pilot rate.
- Now, consider the MIT decoder curves for a chosen RSCC memory. Pick the curve with the most puncturing (smallest K) for which the output MI is 1 for an input MI of $\mathrm{MI}_{\mathrm{equ}}^{\max}$. Hence we have determined the puncturing rate K.
- The pilot rate can then be chosen as frequent as possible (smallest P) while still satisfying the desired data and symbol rates. By doing this the number of turbo iterations will be minimized.

7 Conclusion

In this paper have used EXIT charts to analyze an adaptive turbo equalization receiver in fast-fading channels. The receiver comprised an expanded trellis APP equalizer and an APP RSCC decoder. We have shown that the maximum output MI of the TE-APP equalizer is independent of the pilot rate, and is determined only by the SNR and the fading rate. We also examined the tradeoff between code puncturing and pilot insertion while maintaining constant data and symbol rates. Finally we proposed new design procedures for adaptive turbo equalizers based on our EXIT chart analysis.

References

[1] R. Raheli, A. Polydoros, and C.-K. Tzou, "Per-survivor processing: A general approach to MLSE in uncertain environments," *IEEE Trans. on Communications*, vol. 43, pp. 354–364, Feb 1995.

[2] J. K. Cavers, "An analysis of pilot symbol assisted modulation for Rayleigh fading channels," *IEEE Trans. on Vehicular Technology*, vol. 40, pp. 686–693, Nov. 1991.

[3] J. Han and C. Georghiades, "Maximum-Likelihood Sequence Estimation for Fading Channels via the EM Algorithm," in *Proc. GLOBECOM'93*, vol. 4, (Houston), pp. 133–137, 1993.

[4] L. Davis, I. Collings, and P. Hoeher, "Joint MAP Equalization and Channel Estimation for Frequency-Selective and Frequency-Flat

Fast-Fading Channels," *IEEE Trans. on Communications*, vol. 49, pp. 2106–2114, Dec. 2001.

[5] C. Laot, A. Glavieux, and J. Labat, "Turbo Equalization: Adaptive Equalization and Channel Decoding Jointly Optimized," *IEEE Journal on Selected Areas in Communications*, vol. 19, pp. 1744–1752, Sept. 2001.

[6] L. R. Bahl, J. Cocke, F. Jelinek, and J. Raviv, "Optimal Decoding of Linear Codes for Minimizing Symbol Error Rate," *IEEE Trans. on Information Theory*, vol. 20, pp. 284–287, Mar. 1974.

[7] S. ten Brink, "Convergence Behavior of Iteratively Decoded Parallel Concatenated Codes," *IEEE Trans. on Communications*, vol. 49, pp. 1727 –1737, Oct. 2001.

[8] I. Land and P. Hoeher, "Using the Mean Reliability as a Design and Stopping Criterion for Turbo Codes," in *Proc. ITW'01*, pp. 27–29, Sept. 2001.

[9] J. Hagenauer, "Log-Likelihood Ratios, Mutual Information and EXIT Charts - a Primer," in *Proc. 12th Joint Conference on Communication and Coding*, (Saas Fe, Switzerland), Mar. 2002.

[10] S. Dolinar and D. Divsalar, "Weight Distributions for Turbo Codes Using Random and Nonrandom Permutations," tech. rep., TDA Progress Report 42-122, Aug. 1995.

[11] CEPT/ETSI, "GSM recommendations," Tech. Rep. 05.05, Annex 3., ETSI, Nov. 1988.

[12] A. Picart, P. Didier, and A. Glavieux, "Turbo-Detection: A New Approach to Combat Channel Frequency Selectivity," in *IEEE Conference on Communications (ICC)*, vol. 3, (Montreal, Canada), pp. 1498–1502, June 1997.

[13] D. Raphaeli and Y. Zarai, "Combined Turbo Equalization and Turbo Decoding," *IEEE Communications Letters*, vol. 2, pp. 107–109, Apr. 1998.

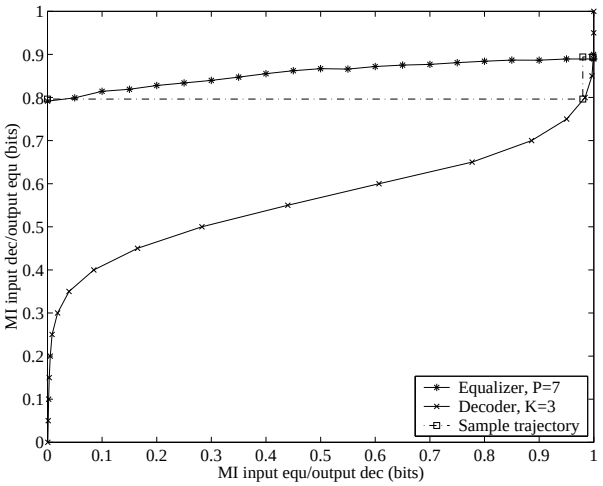

Figure 5. Example EXIT chart for adaptive turbo equalizer at 10.5dB SNR

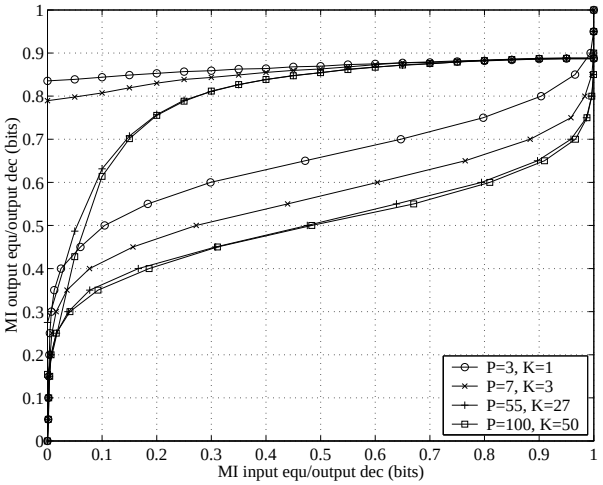

Figure 6. EXIT charts for a fixed redundancy of 0.5 at 10.5dB SNR

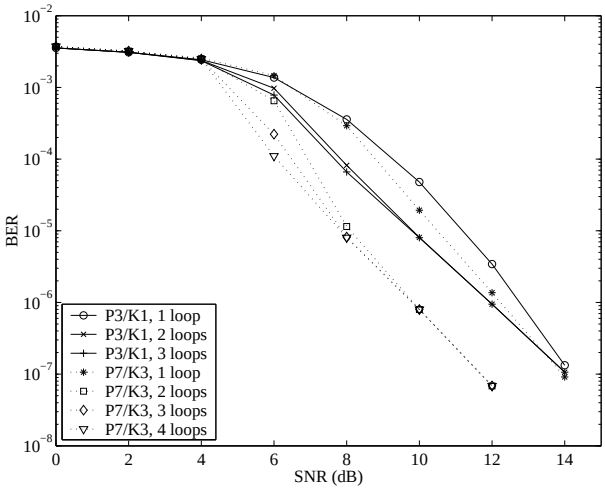

Figure 7. BER vs SNR for adaptive turbo equalizer